



Electrodeposited Platinum Iridium Enables Microstimulation With Carbon Fiber Electrodes

Elena della Valle^{1,2*}, Beomseo Koo^{1,2}, Paras R. Patel^{1,2}, Quentin Whitsitt³, Erin K. Purcell³, Cynthia A. Chestek^{1,2,4,5,6} and James D. Weiland^{1,7,2}

¹Biomedical Engineering Department, University of Michigan, Ann Arbor, MI, United States, ²Biointerfaces Institute, University of Michigan, Ann Arbor, MI, United States, ³College of Engineering, Michigan State University, East Lansing, IN, United States, ⁴Department of Electrical Engineering and Computer Science, University of Michigan, Ann Arbor, MI, United States, ⁵Robotics Graduate Program, University of Michigan, Ann Arbor, MI, United States, ⁶Neuroscience Graduate Program, University of Michigan, Ann Arbor, MI, United States, ⁷Department of Ophthalmology and Visual Sciences, Kellogg Eye Center, University of Michigan, Ann Arbor, MI, United States

OPEN ACCESS

Edited by:

Hui Fang,
Dartmouth College, United States

Reviewed by:

Hyowon Lee,
Purdue University, United States
Wonryung Lee,
Korea Institute of Science and
Technology, South Korea
Yongli Qi,
Dartmouth College, United States

*Correspondence:

Elena della Valle
eldellav@umich.edu

Specialty section:

This article was submitted to
Nanodevices,
a section of the journal
Frontiers in Nanotechnology

Received: 24 September 2021

Accepted: 10 November 2021

Published: 02 December 2021

Citation:

della Valle E, Koo B, Patel PR,
Whitsitt Q, Purcell EK, Chestek CA and
Weiland JD (2021) Electrodeposited
Platinum Iridium Enables
Microstimulation With Carbon
Fiber Electrodes.
Front. Nanotechnol. 3:782883.
doi: 10.3389/fnano.2021.782883

Ultrasmall microelectrode arrays have the potential to improve the spatial resolution of microstimulation. Carbon fiber (CF) microelectrodes with cross-sections of less than 8 μm have been demonstrated to penetrate cortical tissue and evoke minimal scarring in chronic implant tests. In this study, we investigate the stability and performance of neural stimulation electrodes comprised of electrodeposited platinum-iridium (PtIr) on carbon fibers. We conducted pulse testing and characterized charge injection *in vitro* and recorded voltage transients *in vitro* and *in vivo*. Standard electrochemical measurements (impedance spectroscopy and cyclic voltammetry) and visual inspection (scanning electron microscopy) were used to assess changes due to pulsing. Similar to other studies, the application of pulses caused a decrease in impedance and a reduction in voltage transients, but analysis of the impedance data suggests that these changes are due to surface modification and not permanent changes to the electrode. Comparison of scanning electron microscope images before and after pulse testing confirmed electrode stability.

Keywords: carbon fiber microelectrode (CFME), PtIr coating, microstimulation, *in vivo* stimulation, *in vitro* stimulation

1 INTRODUCTION

Ultramicroelectrodes are a class of neural interfaces distinguished by cross-sectional dimensions of less than 15 microns. Ultramicroelectrodes include carbon fiber arrays (Patel et al., 2015; Welle et al., 2020), the Neurolace and NET probes (Xie et al., 2015), silicon carbide microelectrodes (SiC) (Deku et al., 2018), high density microwires (Kollo et al., 2020), and 3D printed arrays (Ali et al., 2021). These devices drastically reduce the foreign body reaction compared to penetrating arrays with larger features (Polikov et al., 2005). The small size of ultramicroelectrodes makes them challenging to utilize since they either lack the stiffness to penetrate the brain (and require a temporary stiffener) or are brittle and thus difficult to handle. Polyimide is an example of an electrode substrate that requires a stiffener while silicon is an example of an electrode that is stiff but brittle at dimensions below 15 microns. Carbon fiber (CF) ultramicroelectrodes have proven to be strong enough to penetrate the cortex (Patel et al., 2015; Patel et al., 2016; Massey et al., 2019) and peripheral nerve (Gillis et al., 2018; Dehdashtian et al., 2020) yet small enough to evoke minimal foreign body reaction (Deku et al., 2018;

Kozai et al., 2012; Patel et al., 2016; Welle et al., 2020, 2021). Since carbon is also conductive, it can serve as both a mechanical substrate and electrical conductor for an ultramicroelectrode (Kozai et al., 2012; Patel et al., 2016; Jiman et al., 2020). However, carbon is not efficient for neural stimulation. This limitation, along with the small dimensions of ultramicroelectrodes, requires enhancement of carbon by coating with an additional material suitable for neural stimulation.

Platinum and platinum-iridium are widely used for neural stimulation (Cogan, 2008). Due to their proven efficiency and stability, these materials are used in clinical devices such as deep brain stimulators, which use macroelectrodes (millimeter dimensions), and therefore can stay within charge density limits ($30 \mu\text{C}/\text{cm}^2$ (Cogan et al., 2016)), and still provide therapeutic levels of stimulation. However, the smaller electrodes site sizes used by ultramicroelectrodes may require a charge density above this limit to evoke responses from cortical cells. Motivated by this need, several alternative materials with improved charge injection capability have been developed. Porous titanium nitride (TiN) has shown biocompatibility and stability along with large charge-injection capacities due to surface roughness. However, accessing the full charge storage capacity under the high current density of neural stimulation is limited by the pore resistance (Posey and Morozumi, 1966; Goldberg et al., 1972; Norlin et al., 2004). The porous platinum known as “Pt gray” can inject a charge density of $1.4 \text{ mC}/\text{cm}^2$ (Zhou, 2005; Zhou, 2011; Fan et al., 2020) without causing material damage or irreversible reactions. Nanostructured platinum (nanoPt) has been recently investigated (Boehler et al., 2020; Wang et al., 2021) through *in vitro* and *in vivo* testing as a potential electrochemical coating both for neural recording and stimulation. Reproducibility of the coating process and stimulation performance for small microelectrodes (cross-section $< 100 \mu\text{m}$) has not been evaluated yet. Hydrated Ir oxide films as activated or sputtered iridium oxide (AIROF or SIROF respectively) have reported high charge injection capabilities (Beebe and Rose, 1988; Klein et al., 1989) in the range of $1\text{--}5 \text{ mC}/\text{cm}^2$. Further, poly (3,4-ethylenedioxythiophene) polystyrene sulfonate (PEDOT—PSS) has shown a charge injection capacity three times higher than AIROF or SIROF (Cogan et al., 2007) although PEDOT stability and robustness remain questionable (Dupont et al., 2014; Welle et al., 2020). Electrodeposited platinum iridium (PtIr) has demonstrated reduced impedance (Cassar et al., 2019; Welle et al., 2020; Della Valle et al., 2021) and lower voltage transients during pulsed current stimulation (Lee et al., 2018), compared to uncoated control electrodes. A recent study (Dalrymple et al., 2019) made a direct comparison between electrodeposited PtIr, reduced graphene oxide, and conducting hydrogel electrodes, finding that PtIr retained low impedance after pulse testing, while graphene failed and conducting hydrogel impedance trended higher. In our previous work (Della Valle et al., 2021) we analyzed the coating morphology of PtIr coated CFs and demonstrated a good coating adhesion during accelerated soak testing.

Here we evaluate CF microelectrode arrays coated with electrodeposited PtIr (PtIr-CF) under conditions of *in vitro* pulse testing at rates of 300 Hz (Chen et al., 2020) and 10 kHz (Kapural et al., 2015), which are of interest in neural engineering, specifically for visual cortex stimulation and high frequency spinal cord stimulation respectively. We characterized PtIr-CF electrodes with electrochemical impedance spectroscopy (EIS), cyclic voltammetry (CV), voltage transients (VT), and scanning electron microscopy (SEM) before and after the coating as well as before and after *in vitro* pulsing tests. Voltage transients were stable during the pulsing process and no delamination was apparent in pulsed electrodes. We also report data from two pilot studies: *in vitro* pulse testing of cellular scale PtIr-CF electrode and *in vivo* pulsing conducted in the visual cortex of a single animal.

2 MATERIALS AND METHODS

2.1 Carbon Fibers Microelectrode Arrays Fabrication

The carbon fiber electrode arrays (CFEA) consist of eight sharpened CFs coated with a Parylene C insulation layer (800 nm) and are attached to a small printed circuit board [ZIF Probe, ZIF, (Patel et al., 2016)]. Insulation is removed at the tip using a blowtorching process (Welle et al., 2021) to expose $100\text{--}150 \mu\text{m}$ of carbon with sharpened tips. The final tip diameter tapers from 8.4 to $\sim 2 \mu\text{m}$ diameter at the tip.

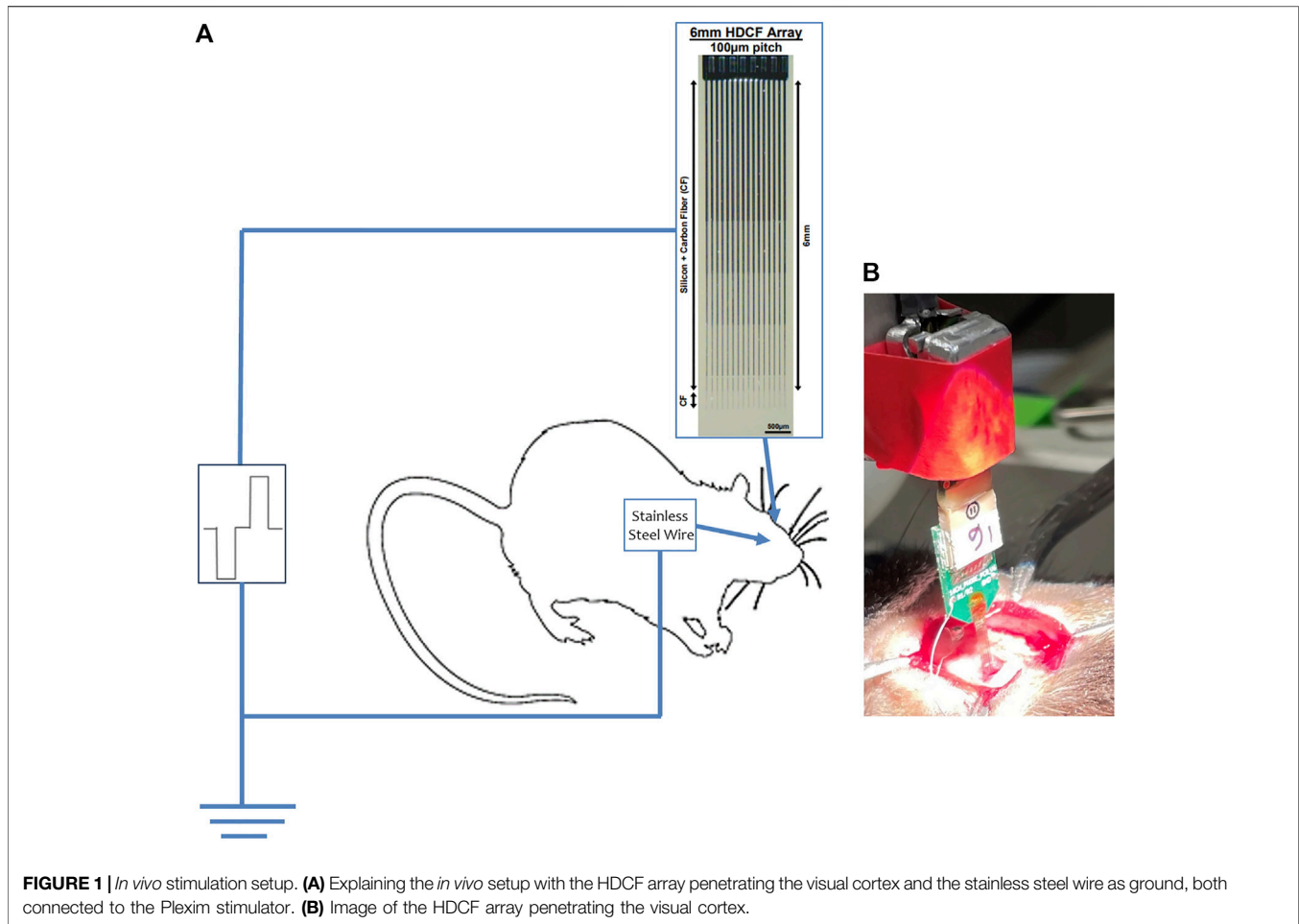
One ZIF with 8 CFs with a small tip exposure was used for the pilot study of *in vitro* pulsing tests of cellular scale PtIr-CF. For the tip preparation of these CFs, instead of the blowtorching method, a scissor was used to expose the CF at the tip. Once cut, the CFs were coated with PtIr (area of $\sim 108 \mu\text{m}^2$, see inset of Figure 7A).

For *in vivo* pulsing tests, one high density carbon fiber (HDCF) array was used. The HDCF fabrication is described elsewhere (Huan et al., 2021). Briefly, the array consisted of 16 silicon shanks of 6 mm length with approximately $250 \mu\text{m}$ of CF protruding from the end of each shank. Parylene-C was used as an insulation layer and the CF tips were blowtorched to expose and sharpen the CF tips, exposing $\sim 100\text{--}150 \mu\text{m}$.

2.2 Electrochemical Impedance Spectroscopy and Cyclic Voltammetry

EIS was collected by applying a 10 mV (peak) sine wave in a frequency range of 1 MHz–10 Hz. All EIS and CV measurements were performed in 1x PBS (0.01 M phosphate buffered saline) solution in a three electrode configuration at open circuit potential using a PtIr wire electrode ($\sim 70 \mu\text{m}$) as counter and an Ag/AgCl as reference electrode (3M NaCl, BASi, West Lafayette, IN, United States). A Gamry 600+ potentiostat (Gamry Inc., Warminster, PA, United States) was used for measurement collection.

Cyclic voltammetry (CV) measurements were obtained by sweeping three times between -0.6 and 0.8 V versus Ag/AgCl at a scan rate of $500 \text{ mV}/\text{s}$. CVs were measured to establish the



cathodal charge storage capacity (CSC_C) (Cogan, 2008). We calculated CSC_C from the time integral of the cathodic current.

2.3 Pt-Ir Electrochemical Deposition

PtIr coatings were electrodeposited using a potential cycling technique in a solution of 0.2 g/L of $\text{Na}_3\text{IrCl}_6\text{H}_2\text{O}$ and 0.186 g/L of $\text{Na}_2\text{PtCl}_6\text{H}_2\text{O}$ in 0.1 M of nitric acid (HNO_3) (Della Valle et al., 2021). A constant temperature of 56°C and a pulsed sonication at a power of 2 W ($T_{ON} = 1$ min and $T_{OFF} = 30$ sec.) were used. A 70 µm PtIr wire (A-M System, Sequim, WA, United States) electrode and an Ag/AgCl (3M NaCl, BASi, West Lafayette, IN, United States) were used as counter and reference electrode respectively. The potential range for the electrodeposition process was -0.1 to 0.1 V with 200 mV/s of scan rate for 1,200 cycles, which corresponds to a coating process time of 45 min. A Gamry 600+ potentiostat (Gamry Instruments, Warminster, PA, United States) was used to apply potential cycles and an A700 Qsonica (Qsonica L.L.C. Newtown, CT, United States) was used for sonication.

2.4 SEM Images Acquisition

Images of CFs were acquired with scanning electron microscopy (SEM) before coating, after coating, and after pulse testing, using

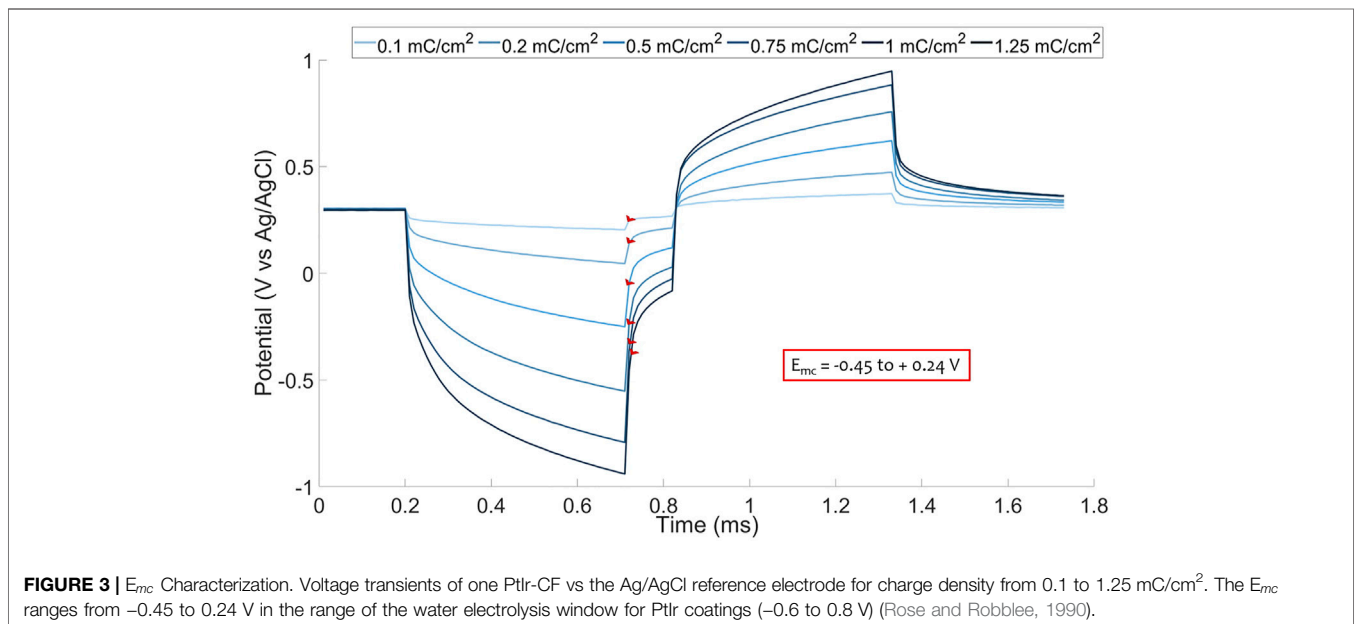
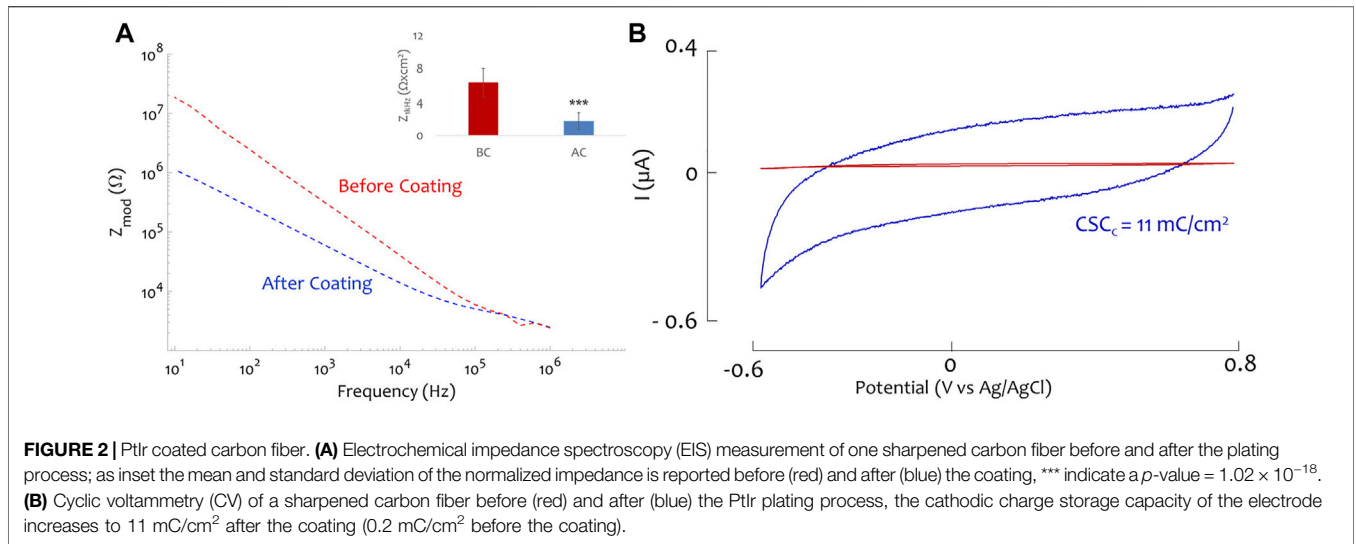
a Tescan Rise SEM (Tescan Orsay Holding, Brno—Kohoutovice, Czech Republic) in low vacuum mode (LVSTD, low vacuum secondary electron detector). Low vacuum mode allows imaging without deposition of a conductive film (i.e., gold). Samples were mounted on SEM stubs with the conductive carbon tape without the CF touching the tape. An excitation voltage between 5 and 20 kV was used.

2.5 In-vitro Pulse Testing

2.5.1 300 Hz and 10 kHz *In Vitro* Pulsing Test

A PlexStim Electrical Stimulator System (Plexon, Dallas, TX, United States, software version 2.3) was used to deliver cathodic first biphasic electric pulses with a charge density of 1 mC/cm². A bipolar stimulation was done choosing as ground one PtIr-CF on the pulsed CFEA. Two different current amplitude and pulse duration were applied on the sharp carbon fibers:

- 1) Electric pulses with a duration of 170 µs, interphase of 60 µs at a frequency of 300 Hz. Pulsing tests were conducted for 12 h (~13 million pulses);
- 2) Electric pulses with 30 µs of duration at a frequency of 10 kHz for 3 h (~108 million pulses).



EIS measurements were taken before and after electric pulsing tests. All the experiments were conducted at room temperature. SEM images were collected before and at the end of pulsing tests to determine surface modifications due to the electric stimulation. The PlexStim provides single ended outputs of the current waveform (presented as a voltage across a resistor) and the VT across the test and counter electrodes. The current and the VT were monitored both for *in vitro* and *in vivo* pulsing tests, using a digital oscilloscope (Tektronix TBS 1032B, Beaverton, OR, United States). The electrochemical cell used consisted of a petri dish (Millipore Sigma, diameter of 80 mm and a volume of $\sim 75 \text{ ml}$) containing 1x of a PBS solution; the leads of the stimulator were connected to the pulsed carbon fiber, and the ground connected to one of the CFs of the pulsed ZIF board.

2.5.2 Electrode Polarization

A three electrode configuration method was used to measure the maximum cathodic polarization, E_{mc} of PtIr-CF electrode (Cogan, 2008). For that purpose, we used the chronoamperometry experiment of the Gamry potentiostat. An Ag/AgCl and a large Pt foil ($5 \times 9 \text{ mm}^2$) were used as reference and counter electrodes respectively. Biphasic cathodic first current pulses of duration of $500 \mu\text{s}$ and charge intensity from 0.1 to 1.25 mC/cm^2 were applied.

2.5.3 *In vitro* Cellular Scale PtIr-CF Pulsing Test

One ZIF board with eight small PtIr-CFs (section 2.1 for fabrication details) was characterized by means of pulsing tests. A PlexStim Electrical Stimulator System (Plexon, Dallas, TX, United States, software version 2.3) was used to deliver

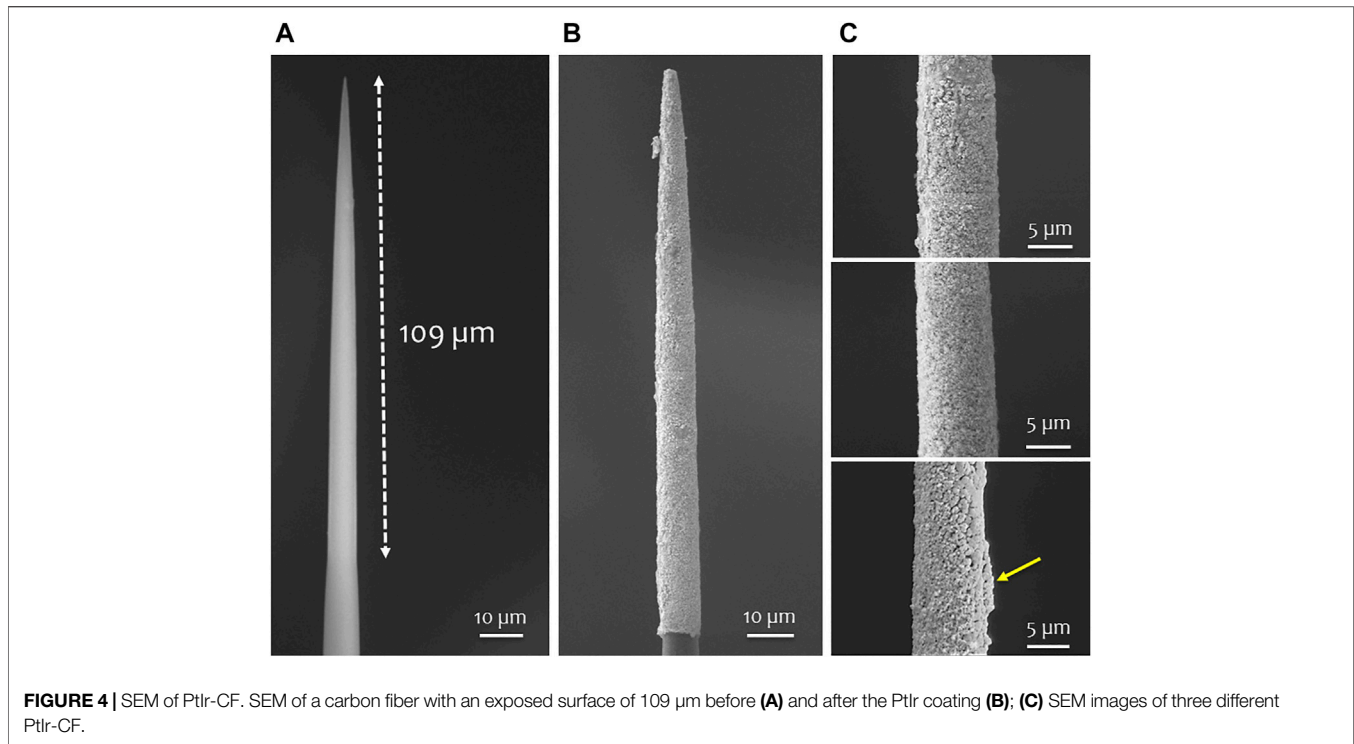


TABLE 1 | Mean and standard deviation of the normalized impedance at 1 kHz, list of all components extracted from the equivalent circuit model (see inset of Figure 5A), VT_{peak} for Day 1 and Day 2 before and after pulsing. The p -value from the paired t-test are reported with a significance difference for the constant phase element components as well as for normalized impedance at 1 kHz and the VT_{peak} before and after pulsing on Day 1 and Day 2.

	$Z_{1\text{kHz}} \Omega\text{cm}^2$	$Ru (\Omega)$	$Y0 (\text{S}\cdot\text{s}^n)$	α	$C (F)$	VT_{peak}
BP_{Day1}	0.69 ± 0.1	$6.8 \pm 2.1 \times 10^3$	$2.13 \pm 0.86 \times 10^{-7}$	0.58 ± 0.05	$5.01 \pm 0.94 \times 10^{-11}$	1.19 ± 0.08
AP_{Day1}	0.27 ± 0.02	$6.2 \pm 0.74 \times 10^3$	$2.9 \pm 1.1 \times 10^{-7}$	0.7 ± 0.05	$5.48 \pm 0.68 \times 10^{-11}$	0.94 ± 0.1
$p\text{-value}_{Day1}$	7.45×10^{-5}	0.33	0.003	1.29×10^{-5}	0.25	9×10^{-7}
BP_{Day2}	0.6 ± 0.13	$6.7 \pm 1.5 \times 10^3$	$2.7 \pm 0.8 \times 10^{-7}$	0.49 ± 0.05	$5.45 \pm 1 \times 10^{-11}$	1.1 ± 0.11
AP_{Day2}	0.25 ± 0.04	$6 \pm 1.1 \times 10^3$	$3.63 \pm 1.2 \times 10^{-7}$	0.7 ± 0.05	$5.4 \pm 1.7 \times 10^{-11}$	0.93 ± 0.1
$p\text{-value}_{Day2}$	6.41×10^{-6}	0.07	0.0026	2.15×10^{-5}	0.97	0.0014

cathodic first biphasic electric pulses with a duration and interphase gap of 100 μs at 100 Hz. Current amplitudes ranged from 5 to 20 μA . The pulse was applied for the duration of 1 min per CF. A 70 μm PtIr wire was used as the counter electrode.

2.6 In vivo Pulsing Tests

2.6.1 High Density Carbon Fiber Array Fabrication

One HDCF (section 2.1 for details) array was used for *in vivo* visual cortex stimulation. The HDCF used for this experiment consisted of four CF electrodes, one coated CF for pulse testing and three for stab controls, with the remaining 12 fibers removed for easier insertion.

2.6.2 Rat Surgery

The surgical procedure used was approved by the Michigan State University Animal Care and Use Committee. One Sprague-Dawley rat was anesthetized with 3% isoflurane and maintained at 1–3%. Once hind-limb pinch response was muted, the rat's head was shaven and placed on a stereotaxic

with an anesthesia nosecone, and the head was fixed with ear bars. A longitudinal incision was made at the dorsal surface of the animal's head, the fascia was removed, and the exposed skull was cleaned and dried. Excessive bleeding of the skull or surrounding skin was stopped with either absorbent spear or cauterization. A 3 \times 3 mm craniotomy at the primary visual cortex (V1) was made using this coordinate: (Anterior-Posterior, Medial-Lateral) (–6.5, –3.5) mm from Bregma.

2.6.3 In vivo Stimulation Protocol

For *in vivo* stimulation, the dura was removed and the PtIr-HDCF was driven into the cortex until a depth of 300 μm was reached. An 8 cm stainless steel wire (A-M Systems) was used as a stimulation return electrode. One minute after insertion, the PtIr-HDCF was connected to the Plexon PlexStim system, and the stimulation return electrode was sutured under the loose skin at the incision site using vicryl sutures. Cathodic-first, symmetric-biphasic pulses with 200 μs duration per phase, 100 μs interphase gap, and 50 Hz pulse frequency were used with four amplitudes:

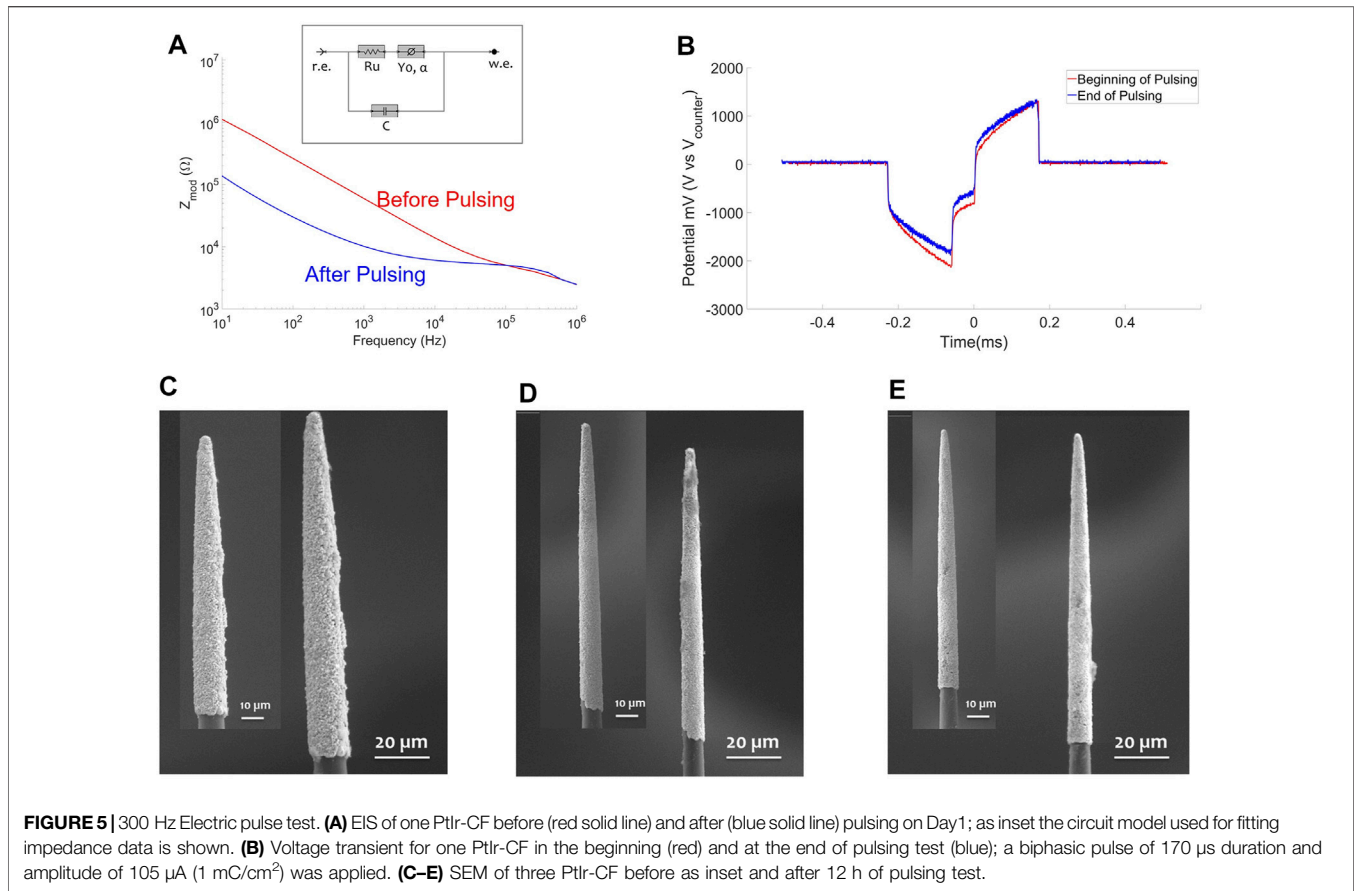


FIGURE 5 | 300 Hz Electric pulse test. **(A)** EIS of one PtIr-CF before (red solid line) and after (blue solid line) pulsing on Day 1; as inset the circuit model used for fitting impedance data is shown. **(B)** Voltage transient for one PtIr-CF in the beginning (red) and at the end of pulsing test (blue); a biphasic pulse of 170 μ s duration and amplitude of 105 μ A (1 mC/cm²) was applied. **(C–E)** SEM of three PtIr-CF before as inset and after 12 h of pulsing test.

10, 15, 20, 25 μ A (from 0.1 to 0.3 mC/cm²). 6,000 pulses were applied for each current amplitude. After collection of VT, the electrode was driven further into the tissue until 600 μ m, and the tissue was stimulated for a total of 1 h (~180k pulses) at 25 μ A (0.3 mC/cm²) and 5 μ s interphase gap. VTs were collected every 10 minutes.

The summary image shown in **Figure 1A** explains the *in vivo* setup, with the HDCF array penetrating the visual cortex and the stainless steel wire as the counter electrode.

2.7 Statistical Analysis and Electric Circuit Model

A paired t-test was used to compare impedance data for CF and PtIr-CF as well as to compare CSC_C prior to and after the coating. A paired t-test was also applied to impedance data before and after pulsing both at 300 and 10 kHz. One paired t-test was done for comparing the VT_{peak} of the VT at the beginning and at the end of each pulse test.

Impedance before and after pulsing at both 300 Hz and 10 kHz were fitted to a circuit model (see inset of **Figure 5A**). The circuit model consisted of a reference electrode (r.e.), the electrolyte resistance (Ru), the admittance (Y0), and the exponent (α) of the constant phase element (CPE), the parasitic capacitance (C), and the working electrode (w.e.). The extracted parameters were

statistically analyzed using a paired t-test. For all the statistical tests, Matlab R2021a was used.

3 RESULTS

3.1 PtIr Coating Protocol Assessment

A total of 39 blowtorched CFs (distributed across five ZIF Boards) were coated with PtIr. The surface area was estimated by SEM inspection and ranged from 1900 to 3,600 μ m². The impedance data were normalized by the electrode area ($\Omega \times$ cm²). An average 1 kHz normalized impedance and standard deviation of $1.74 \pm 0.98 \Omega \times$ cm² was measured for PtIr-CF. **Figure 2A** shows a representative impedance spectrum from before and after PtIr coating and average data at 1 kHz, normalized to surface area. A significant decrease (*p*-value of 1.02×10^{-18}) in 1 kHz impedance is noted, while impedance above 100 kHz state is unchanged, indicating no change in geometric surface area.

In **Figure 2B**, the cyclic voltammetry (CV) is reported for one CF prior (red) and after the PtIr coating. From the CV, the CSC_C (Cogan, 2008) can be quantified. In the example reported in **Figure 2B** the PtIr enhanced the CSC_C from 0.2 to 11 mC/cm². CV was done for 21 CFs and the mean and standard deviation of the CSC_C was of 0.25 ± 0.13 mC/cm² and 13.1 ± 8.74 mC/cm² for

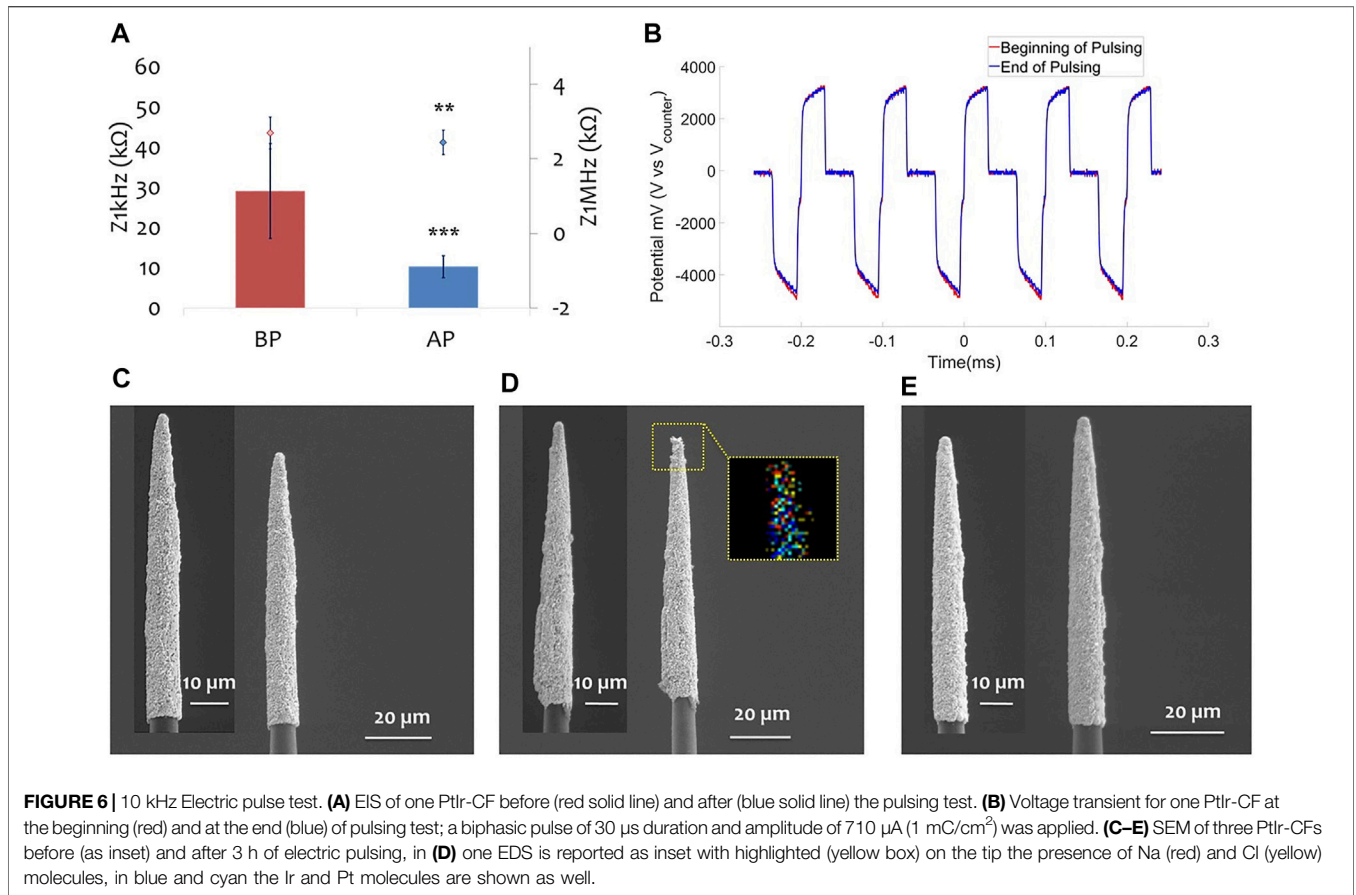


FIGURE 6 | 10 kHz Electric pulse test. **(A)** EIS of one PtIr-CF before (red solid line) and after (blue solid line) the pulsing test. **(B)** Voltage transient for one PtIr-CF at the beginning (red) and at the end (blue) of pulsing test; a biphasic pulse of 30 μ s duration and amplitude of 710 μ A (1 mC/cm²) was applied. **(C–E)** SEM of three PtIr-CFs before (as inset) and after 3 h of electric pulsing, in **(D)** one EDS is reported as inset with highlighted (yellow box) on the tip the presence of Na (red) and Cl (yellow) molecules, in blue and cyan the Ir and Pt molecules are shown as well.

TABLE 2 | Mean and standard deviation of the normalized impedance at 1 kHz, list of all components extracted from the equivalent circuit model reported as inset in **Figure 5A**, VT_{peak} before and after pulsing. The p -values from the paired t-test are reported with a significance difference for the α value of the CPE and for both normalized impedance and VT_{peak} .

	$Z_{1kHz} \Omega \times cm^2$	$R_u (\Omega)$	$Y_0 (S \cdot s^\alpha)$	α	$C (F)$	VT_{peak}
BP	0.58 ± 0.21	$6.1 \pm 1.9 \times 10^3$	$3.4 \pm 1.77 \times 10^{-7}$	0.58 ± 0.07	$5.01 \pm 0.94 \times 10^{-11}$	2.99 ± 0.37
AP	0.21 ± 0.05	$5.9 \pm 0.6 \times 10^3$	$4.3 \pm 1.9 \times 10^{-7}$	0.73 ± 0.09	$5.48 \pm 1.4 \times 10^{-11}$	2.74 ± 0.33
p -value	0.00017	0.77	0.14	7×10^{-4}	0.24	0.002

the CF and PtIr-CF respectively. A paired t-test revealed a statistically significant difference with a p -value of 1.62×10^{-6} .

To determine the E_{mc} (Cogan, 2008), PtIr-CF were characterized as described in **section 2.5.2**. In **Figure 3** the VT are reported with a Eipp (bias level (Cogan, 2008)) of 0.3 V and an E_{mc} ranging from -0.45 to 0.24 V in the range of the water electrolysis window for PtIr electrodes of -0.6 to 0.8 V (Rose and Robblee, 1990).

SEM images were collected before and after the coating process. One example of a CF and a PtIr-CF is reported in **Figures 4A,B** respectively. The PtIr-CF surface appears homogeneously coated. Detailed SEM of three PtIr-CFs are shown in **Figure 4C** highlighting a rough, continuous coating. Some surface irregularities are also noted (see yellow arrow of **Figure 4C**). Adjacent CFs can become temporarily in contact

during the plating process, which results in a ridge of PtIr along one side.

EDS was done to evaluate the Pt and Ir percentage of the PtIr-CF surface. A percentage of 66% for Pt and 34% was measured on one PtIr-CF, consistent with results obtained in a previous set of coated electrodes (Della Valle et al., 2021).

3.2 Electric Pulsing Tests

3.2.1 300 Hz Electric Pulsing Tests

PtIr-CFs ($N = 10$, area ranging from 1900 to 2,100 μ m²) were tested by applying biphasic cathodic first electric pulses of 170 μ s duration at a frequency of 300 Hz (Chen et al., 2020) with a charge density of 1 mC/cm² for 12 h on two consecutive days (6 h each day). In **Figure 5A** the impedance for one PtIr-CF is reported before (red solid line) and after (blue solid line)

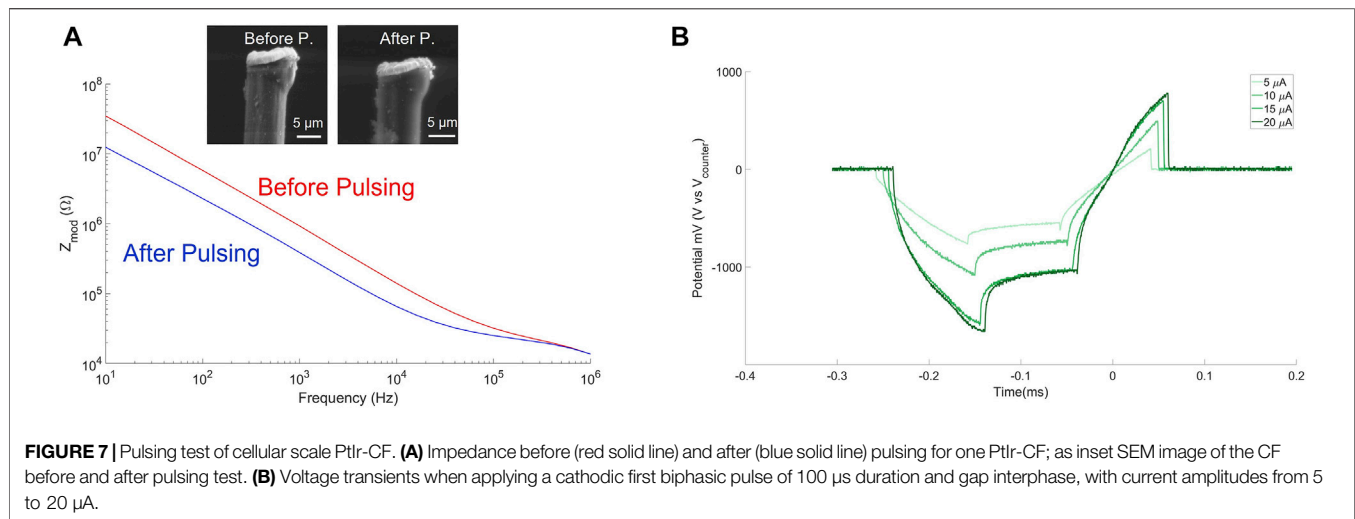


FIGURE 7 | Pulsing test of cellular scale PtIr-CF. **(A)** Impedance before (red solid line) and after (blue solid line) pulsing for one PtIr-CF before and after pulsing test. **(B)** Voltage transients when applying a cathodic first biphasic pulse of 100 μ s duration and gap interphase, with current amplitudes from 5 to 20 μ A.

pulsing test on Day 1. An impedance decrease after the pulsing test was obtained for all pulsed PtIr-CFs on both days. Similar decreases in impedance after pulsing have been attributed to the modification of the electrode surface (Fomani and Mansour, 2011; Vomero et al., 2017). In **Table 1** the mean, the standard deviation, and the p -value of the normalized impedance at 1 kHz is reported before and after pulsing on both days. The 1 kHz impedance variation before and after pulsing was statistically significant on both Day 1 and Day 2. To further analyze the impedance variation before and after pulsing, a circuit model (see inset in **Figure 5A**) was fitted and a paired t -test was applied to the extracted parameters. In **Table 1** the mean and standard deviation for the extracted parameters is reported with the associated p -value both for Day 1 and Day 2 of pulsing tests. The CPE components values changed, but R_u was not significantly different before and after pulsing. This further supports the finding that pulsing modified the surface of the electrode (Y_0 changed), but did not change the geometric shape (R_u unchanged). No geometric modification was further confirmed by the SEM images shown in **Figures 5C–E**. NaCl aggregation was noticed (**Figure 5D**) on the coated surface and confirmed by EDS (data not shown).

VT were monitored during the pulsing test. One example is shown in **Figure 5B**, in red and blue are reported VT for Day 1 at the beginning and end of the pulsing tests (6 h) respectively. In **Table 1** the mean and standard deviation of the VT_{peak} are reported for Day 1 and Day 2 of pulsing tests. The p -values from the paired t -test were statistically significant for both days (**Table 1**).

3.2.2 10 kHz Electric Pulse Tests

PtIr-CFs ($N = 10$, area ranging from 1,700 to 2,100 μm^2) were tested at a frequency of 10 kHz (Kapural et al., 2015) by applying biphasic cathodic first electric pulses of 30 μ s duration and a charge density of 1 mC/cm^2 for 3 h.

In **Figure 6A** the EIS of one PtIr-CF before (red solid line) and after (blue solid line) pulsing is reported. As in the 300 Hz pulsing test, a significant reduction of the 1 kHz impedance was found

after pulsing (see **Table 2**). A circuit model (see inset of **Figure 5A**) was fitted to the impedance data prior to and after pulsing tests. In **Table 2** the mean and the standard deviation of the extracted parameters are reported, with a statistically significant difference for the α component of the CPE, which suggests increased capacitive behavior for the electrode surface. The increase in Y_0 was not statistically significant.

VT were monitored for the whole pulsing test and the mean of the VT_{peak} at the beginning and end of pulsing is reported in **Table 2**. The VT_{peak} variation before and after the pulsing test was statistically significant. SEM inspection showed no surface modifications (**Figures 6C–E**), an accumulation of salt was detected on the tip of one fiber, as shown in the yellow box in **Figure 6D** with the corresponding EDS, showing Na and Cl molecules in red and yellow as well as in blue and cyan Ir and Pt molecules.

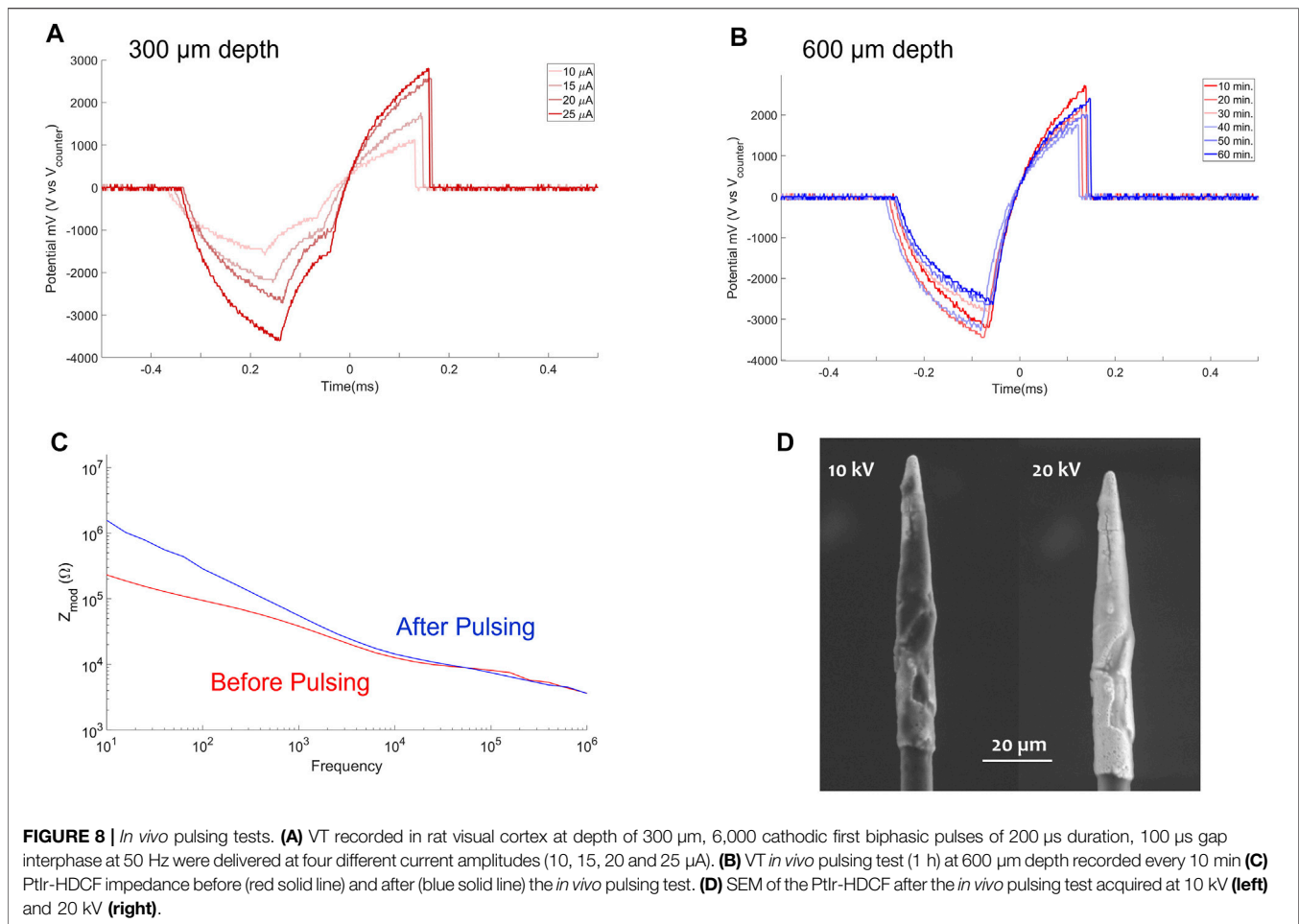
3.2.3 In vitro Cellular Scale PtIr-CF Pulsing Test

In vitro pulsing characterization was done using one ZIF with eight small PtIr-CFs (**section 2.5.3**) to show how electric pulses can be applied using a cellular scale electrode size (less than 15 μm diameter, electrode area of $\sim 108 \mu\text{m}^2$). In **Figure 7A** the impedance before and after pulsing is shown. In **Figure 7B** the voltage transients are reported for each current amplitude applied with a max of 784 mV applied across the electrode surface. No structure modifications occurred as confirmed by the SEM (see inset of **Figure 7A**).

3.3 In vivo Electric Pulsing Test

One HDCF board with one coated CF (PtIr-HDCF, area $\sim 2000 \mu\text{m}^2$) was used to perform pilot tests of *in vivo* electric pulsing test in rat visual cortex. As explained in the method **section 2.6.3**, VT were first collected at 300 μm depth at four different current amplitudes as shown in **Figure 8A**.

Then the PtIr-HDCF was driven at 600 μm of depth into the visual cortex. The tissue was stimulated for a total of 1 h at 25 μA (0.3 mC/cm^2) and 5 μs interphase gap. VTs were collected each 10 min as shown in **Figure 8B**. The mean of the VT_{peak} was of



2.19 ± 0.3 V and a lower VT was recorded at the end of the pulsing test.

In **Figure 8C** the PtIr-HDCF impedance before (red solid line) and after (blue solid line) the *in vivo* pulsing test are reported. After the *in vivo* pulsing test, the impedance magnitude of the PtIrHDCF was slightly increased possibly due to biological tissue adhering on the electrode surface.

SEM were acquired after the *in vivo* pulsing test. In **Figure 8D**, left panel the SEM at 10 kV is reported showing in black, low conductive material adhering on the surface (e.g., biological material). On the right panel of **Figure 8D** the SEM at 20 kV is reported and the PtIr is visible with a crack in the PtIr film near the tip. No SEM was acquired prior to stimulation, so it is unclear when the crack formed. Since the VTs during the *in vivo* experiments were stable, it is more likely that the crack was due to a defect during PtIr deposition or as a result of handling during insertion or SEM preparation.

4 DISCUSSION

The development of small microelectrodes for localized neural stimulation is the key challenge facing neural interfaces. CFEA have proven to effectively provide neural recording from the

motor cortex (Patel et al., 2015, 2016; Massey et al., 2019) as well as from the peripheral nerve (Gillis et al., 2018; Dehdashtian et al., 2020; Welle et al., 2021). We recently (Della Valle et al., 2021) demonstrated how electroplated PtIr can decrease CF impedance with a good coating adherence. However, the stability of PtIr-CFs under electric pulsing test has not been investigated. In the studies presented here, we found PtIr-CFs can inject 1.25 mC/cm^2 (0.5 ms pulses in PBS) while staying within the water window for PtIr. The corresponding current amplitude of 40 μA was well above published activation thresholds for cortical microstimulation (Schmidt et al., 1996). Pulse testing at 300 Hz and 10 kHz resulted in decreases in impedance and voltage transients, consistent with other studies of chronic stimulation (Fomani and Mansour, 2011). This phenomenon does not indicate electrode instability, rather a modification of the surface or cleaning of the exposed electrode area (Fomani and Mansour, 2011; Vomero et al., 2017). Two pilot experiments demonstrated stimulation, with a cellular scale electrode *in vitro* and a sharpened CF in the visual cortex, which also suggests relatively stable electrochemical properties. In all stimulation experiments, visual inspection with SEM found no coating loss or delamination. In general, PtIr-CF appears to be stable for the conditions tested. Our

findings are comparable to other recent work on ultra microelectrodes and materials for microstimulation. Deku et al. (2018) recently developed ultrasmall silicon carbide electrodes (electrode site area from 20 to 200 μm^2) coated either with titanium nitride (TiN) and sputtered iridium oxide films (SIROF) that provided more than 1 nC/ph of charge injection within water electrolysis limits with a 200 μs pulse. Boehler et al. (Boehler et al., 2020) presented nano-structured platinum (nano-Pt) coatings that were able to provide low impedance microelectrodes (ϕ 35 μm) with good electric stability in response to pulsing test both *in vitro* (1.5 billion pulses of 1.5 mC/cm²) and *in vivo* over 5 weeks of implantation for recording and stimulation of mice medial septal nucleus using a 125 μm nano-Pt coated wire. Zheng et al. (2017), characterized 200 μm IrOx nano-Pt microelectrodes *in vitro* as potential stimulating microelectrodes providing a charge density of 1.2 mC/cm².

Finally, voltage transient data measured *in vivo* includes the voltage across both the PtIr-CF electrode and the return electrode. Thus, we did not measure electrode polarization across PtIr-CF *in vivo*. However, it is known that electrode polarization is generally greater *in vivo* (Leung et al., 2014) or in model cerebrospinal fluid (Cogan et al., 2007), versus PBS solution, which we used for electrode polarization measurements (Figure 3). Our VT data showing higher voltage *in vivo* is consistent with these earlier studies. For the same current and pulse width, we found VTs to be two to three times greater *in vivo* vs. *in vitro*. The VT waveforms *in vivo* tend to be rounded, making accurate estimates of polarization difficult. Leung et al. (Leung et al., 2014), determined charge injection limits *in vivo* for retinal, cochlear, and subdural locations, using the same methods for determining charge injection limits *in vitro*. The *in vivo* charge injection limits they found were well below charge density limits found by post-mortem tissue assessment. The authors concluded that *in vivo* charge injection limits cannot be measured in the same manner as *in vitro* tests. EIS taken before and after *in vivo* pulse testing suggested no coating loss on the electrode surface, which was confirmed by SEM. We noted a crack in the coating after *in vivo* stimulation, but this PtIr-CF had no SEM performed prior to pulse testing. Our *in vivo* experiments should be considered preliminary and the next experiments will be augmented with chronic implantation and stimulation, tissue analysis, and imaging data pre and post test implant to determine the safety of stimulation with PtIr-CFs.

REFERENCES

- A. Fomani, A., and Mansour, R. R. (2011). Fabrication and Characterization of the Flexible Neural Microprobes with Improved Structural Design. *Sensors Actuators A: Phys.* 168, 233–241. doi:10.1016/j.sna.2011.04.024
- Ali, M. A., Hu, C., Jahan, S., Yuan, B., Saleh, M. S., Ju, E., et al. (2021). Sensing of COVID-19 Antibodies in Seconds via Aerosol Jet Nanoprinted Reduced-Graphene-Oxide-Coated 3D Electrodes. *Adv. Mater.* 33, 2006647. doi:10.1002/adma.202006647
- Beebe, X., and Rose, T. L. (1988). Charge Injection Limits of Activated Iridium Oxide Electrodes with 0.2 Ms Pulses in Bicarbonate Buffered saline

DATA AVAILABILITY STATEMENT

The raw data supporting the conclusion of this article will be made available by the authors, without undue reservation.

ETHICS STATEMENT

The animal study was reviewed and approved by the Michigan State University Institutional Animal Care and Use Committee (IACUC).

AUTHOR CONTRIBUTIONS

JW contributed to the conception of the study. EDV and JW contributed to the design of the study. EDV performed *in vitro* experiments and data curation. PRP fabricated CF and HDCF arrays. BK and QW performed *in vivo* experiments. All authors contributed to manuscript revision, read, and approved the submitted version.

FUNDING

This work was financially supported by the National Science Foundation (DMR-1625671, NSF award CBET 2129817), by the National Institutes of Health National Institute of Neurological Disorders and Stroke (UF1NS107659), the Office of the Director National Institutes of Health (OT2OD024907), the NSF-funded NeuroNex MINT hub (Multimodal Integrated Neural Technologies) at the University of Michigan under NSF 1707316, the Kellogg Vision Research Core funded by P30 EY007003 from the National Eye Institute, The University of Michigan College of Engineering, the School of Medicine, and Research to Prevent Blindness.

ACKNOWLEDGMENTS

The authors acknowledge the Michigan Center for Materials Characterization and the Lurie Nanofabrication Facility for use of their instruments and staff assistance. The authors acknowledge technical support from Julianna Richie from the Cortical Neural Prosthetics Lab at University of Michigan.

(Neurological Stimulation Application). *IEEE Trans. Biomed. Eng.* 35, 494–495. doi:10.1109/10.2122

- Boehler, C., Vieira, D. M., Egert, U., and Asplund, M. (2020). NanoPt-A Nanostructured Electrode Coating for Neural Recording and Microstimulation. *ACS Appl. Mater. Inter.* 12, 14855–14865. doi:10.1021/acsami.9b22798
- Cassar, I. R., Yu, C., Sambangi, J., Lee, C. D., Whalen, J. J., III, Petrossians, A., et al. (2019). Electrodeposited Platinum-Iridium Coating Improves *In Vivo* Recording Performance of Chronically Implanted Microelectrode Arrays. *Biomaterials* 205, 120–132. doi:10.1016/j.biomaterials.2019.03.017
- Chen, X., Wang, F., Fernandez, E., and Roelfsema, P. R. (2020). Shape Perception via a High-Channel-Count Neuroprosthesis in Monkey Visual Cortex. *Science* 370, 1191–1196. doi:10.1126/science.abd7435

- Cogan, S. F., Ludwig, K. A., Welle, C. G., and Takmakov, P. (2016). Tissue Damage Thresholds during Therapeutic Electrical Stimulation. *J. Neural Eng.* 13, 021001. doi:10.1088/1741-2560/13/2/021001
- Cogan, S. F. (2008). Neural Stimulation and Recording Electrodes. *Annu. Rev. Biomed. Eng.* 10, 275–309. doi:10.1146/annurev.bioeng.10.061807.160518
- Cogan, S., Peramunage, D., Smirnov, A., Ehrlich, J., McCreery, D., and Manookitwongsa, P. (2007). Polyethylenedioxythiophene (PEDOT) Coatings for Neural Stimulation and Recording Electrodes. *Mater. Res. Soc. Meet. Abstr. Q2.7*.
- Dalrymple, A. N., Huynh, M., Robles, U. A., Marroquin, J. B., Lee, C. D., Petrossians, A., et al. (2019). Electrochemical and Mechanical Performance of Reduced Graphene Oxide, Conductive Hydrogel, and Electrodeposited Pt-Ir Coated Electrodes: an Active In Vitro Study. *J. Neural Eng.* 17, 016015. doi:10.1088/1741-2552/ab5163
- Dehdashtian, A., Ursu, D., Patel, P. G., Welle, E., Chestek, C. A., Cederna, P. S., et al. (2020). Abstract 193. *Plast. Reconstr. Surg. - Glob. Open* 8, 131–132. doi:10.1097/01.gox.0000667828.04397.6c
- Deku, F., Cohen, Y., Joshi-Imre, A., Kanneganti, A., Gardner, T. J., and Cogan, S. F. (2018). Amorphous Silicon Carbide Ultramicroelectrode Arrays for Neural Stimulation and Recording. *J. Neural Eng.* 15, 016007. doi:10.1088/1741-2552/aa8f8b
- Della Valle, E., Welle, E. J., Chestek, C. A., and Weiland, J. D. (2021). Compositional and Morphological Properties of Platinum-Iridium Electrodeposited on Carbon Fiber Microelectrodes. *J. Neural Eng.* 8 (5). doi:10.1088/1741-2552/ac20bb
- Dupont, S. R., Novoa, F., Voroshazi, E., and Dauskaradt, R. H. (2014). Decohesion Kinetics of PEDOT:PSS Conducting Polymer Films. *Adv. Funct. Mater.* 24, 1325–1332. doi:10.1002/adfm.201302174
- Fan, B., Rodriguez, A. V., Vercosa, D. G., Kemere, C., and Robinson, J. T. (2020). Sputtered Porous Pt for Wafer-Scale Manufacture of Low-Impedance Flexible Microelectrodes. *J. Neural Eng.* 17, 036029. doi:10.1088/1741-2552/ab965c
- Gillis, W. F., Lissandrillo, C. A., Shen, J., Pearre, B. W., Mertiri, A., Deku, F., et al. (2018). Carbon Fiber on Polyimide Ultra-microelectrodes. *J. Neural Eng.* 15, 016010. doi:10.1088/1741-2552/aa8c88
- Goldberg, I. B., Bard, A. J., and Feldberg, S. W. (1972). Resistive Effects in Thin Electrochemical Cells. Digital Simulations of Electrochemistry in Electron Spin Resonance Cells. *J. Phys. Chem.* 76, 2550–2559. doi:10.1021/j100662a013
- Huan, Y., Gill, J. P., Fritzing, J. B., Patel, P. R., Richie, J. M., della Valle, E., et al. (2021). Carbon Fiber Electrodes for Intracellular Recording and Stimulation. *bioRxiv*.
- Jiman, A. A., Ratze, D. C., Welle, E. J., Patel, P. R., Richie, J. M., Bortorff, E. C., et al. (2020). Multi-channel Intra-neural Vagus Nerve Recordings with a Novel High-Density Carbon Fiber Microelectrode Array. *BioRxiv* 10 (1). doi:10.1038/s41598-020-72512-7
- Kapural, L., Yu, C., Doust, M. W., Gliner, B. E., Vallejo, R., Sitzman, B. T., et al. (2015). Novel 10-kHz High-Frequency Therapy (HF10 Therapy) Is Superior to Traditional Low-Frequency Spinal Cord Stimulation for the Treatment of Chronic Back and Leg Pain. *Anesthesiology* 123, 851–860. doi:10.1097/aln.0000000000000774
- Klein, J. D., Clauson, S. L., and Cogan, S. F. (1989). Morphology and Charge Capacity of Sputtered Iridium Oxide Films. *J. Vacuum Sci. Tech. A: Vacuum, Surf. Films* 7, 3043–3047. doi:10.1116/1.576313
- Kollo, M., Racz, R., Hanna, M.-E., Obaid, A., Angle, M. R., Wray, W., et al. (2020). Chime: Cmos-Hosted In Vivo Microelectrodes for Massively Scalable Neuronal Recordings. *Front. Neurosci.* 14, 834. doi:10.3389/fnins.2020.00834
- Kozai, T. D. Y., Langhals, N. B., Patel, P. R., Deng, X., Zhang, H., Smith, K. L., et al. (2012). Ultrasmall Implantable Composite Microelectrodes with Bioactive Surfaces for Chronic Neural Interfaces. *Nat. Mater.* 11, 1065–1073. doi:10.1038/nmat3468
- Lee, C. D., Hudak, E. M., Whalen, J. J., III, Petrossians, A., and Weiland, J. D. (2018). Low-impedance, High Surface Area Pt-Ir Electrodeposited on Cochlear Implant Electrodes. *J. Electrochem. Soc.* 165, G3015–G3017. doi:10.1149/2.0031812jes
- Leung, R. T., Shivdasani, M. N., Nayagam, D. A., and Shepherd, R. K. (2014). In Vivo and In Vitro Comparison of the Charge Injection Capacity of Platinum Macroelectrodes. *IEEE Trans. Biomed. Eng.* 62, 849–857. doi:10.1109/TBME.2014.2366514
- Massey, T. L., Santacruz, S. R., Hou, J. F., Pister, K. S. J., Carmena, J. M., and Maharbiz, M. M. (2019). A High-Density Carbon Fiber Neural Recording Array Technology. *J. Neural Eng.* 16, 016024. doi:10.1088/1741-2552/aae8d9
- Norlin, A., Pan, J., and Leygraf, C. (2004). Investigation of Electrochemical Behavior of Stimulation/sensing Materials for Pacemaker Electrode Applications: I. Pt, Ti, and Tin Coated Electrodes. *J. Electrochem. Soc.* 152, J7. doi:10.1149/1.1842092
- Patel, P. R., Na, K., Zhang, H., Kozai, T. D. Y., Kotov, N. A., Yoon, E., et al. (2015). Insertion of Linear 8.4µm Diameter 16 Channel Carbon Fiber Electrode Arrays for Single Unit Recordings. *J. Neural Eng.* 12, 046009. doi:10.1088/1741-2560/12/4/046009
- Patel, P. R., Zhang, H., Robbins, M. T., Nofar, J. B., Marshall, S. P., Kobylarek, M. J., et al. (2016). Chronic In Vivo Stability Assessment of Carbon Fiber Microelectrode Arrays. *J. Neural Eng.* 13, 066002. doi:10.1088/1741-2560/13/6/066002
- Polikov, V. S., Tresco, P. A., and Reichert, W. M. (2005). Response of Brain Tissue to Chronically Implanted Neural Electrodes. *J. Neurosci. Methods* 148, 1–18. doi:10.1016/j.jneumeth.2005.08.015
- Posey, F. A., and Morozumi, T. (1966). Theory of Potentiostatic and Galvanostatic Charging of the Double Layer in Porous Electrodes. *J. Electrochem. Soc.* 113, 176. doi:10.1149/1.2423897
- Rose, T. L., and Robblee, L. S. (1990). Electrical Stimulation with Pt Electrodes. Viii. Electrochemically Safe Charge Injection Limits with 0.2 Ms Pulses (Neuronal Application). *IEEE Trans. Biomed. Eng.* 37, 1118–1120. doi:10.1109/10.61038
- Schmidt, E. M., Bak, M. J., Hambrecht, F. T., Kufta, C. V., O'Rourke, D. K., and Vallabhanath, P. (1996). Feasibility of a Visual Prosthesis for the Blind Based on Intracortical Micro Stimulation of the Visual Cortex. *Brain* 119, 507–522. doi:10.1093/brain/119.2.507
- Vomero, M., Castagnola, E., Ciarpella, F., Maggiolini, E., Goshi, N., Zucchini, E., et al. (2017). Highly Stable Glassy Carbon Interfaces for Long-Term Neural Stimulation and Low-Noise Recording of Brain Activity. *Sci. Rep.* 7, 1–14. doi:10.1038/srep40332
- Wang, Y., Graham, S., and Unsworth, C. P. (2021). Superior Galvanostatic Electrochemical Deposition of Platinum Nanograss Provides High Performance Planar Microelectrodes for In Vitro Neural Recording. *J. Neural Eng.* doi:10.1088/1741-2552/ac1bc1
- Welle, E. J., Patel, P. R., Woods, J. E., Petrossians, A., Della Valle, E., Vega-Medina, A., et al. (2020). Ultra-small Carbon Fiber Electrode Recording Site Optimization and Improved In Vivo Chronic Recording Yield. *J. Neural Eng.* 17, 026037. doi:10.1088/1741-2552/ab8343
- Welle, E. J., Woods, J. E., Jiman, A. A., Richie, J. M., Bortorff, E. C., Ouyang, Z., et al. (2021). Sharpened and Mechanically Durable Carbon Fiber Electrode Arrays for Neural Recording. *IEEE Trans. Neural Syst. Rehabil. Eng.* 29, 993–1003. doi:10.1109/tnsre.2021.3082056
- Xie, C., Liu, J., Fu, T.-M., Dai, X., Zhou, W., and Lieber, C. M. (2015). Three-dimensional Macroporous Nanoelectronic Networks as Minimally Invasive Brain Probes. *Nat. Mater.* 14, 1286–1292. doi:10.1038/nmat4427
- Zeng, Q., Xia, K., Sun, B., Yin, Y., Wu, T., and Humayun, M. S. (2017). Electrodeposited Iridium Oxide on Platinum Nanocones for Improving Neural Stimulation Microelectrodes. *Electrochimica Acta* 237, 152–159. doi:10.1016/j.electacta.2017.03.213
- Zhou, D. M. (2005). Platinum Electrode and Method for Manufacturing the Same. *US Patent* 6 (974), 533, 2005. [Dataset].
- Zhou, D. M. (2011). Platinum Electrode Surface Coating and Method for Manufacturing the Same. *US Patent* 7 (887), 681, 2011. [Dataset].

Conflict of Interest: The author JW has a financial interest in PtIr coating.

The remaining authors declare that the research was conducted in the absence of any commercial or financial relationships that could be construed as a potential conflict of interest.

Publisher's Note: All claims expressed in this article are solely those of the authors and do not necessarily represent those of their affiliated organizations, or those of the publisher, the editors, and the reviewers. Any product that may be evaluated in this article, or claim that may be made by its manufacturer, is not guaranteed or endorsed by the publisher.

Copyright © 2021 della Valle, Koo, Patel, Whitsitt, Purcell, Chestek and Weiland. This is an open-access article distributed under the terms of the Creative Commons Attribution License (CC BY). The use, distribution or reproduction in other forums is permitted, provided the original author(s) and the copyright owner(s) are credited and that the original publication in this journal is cited, in accordance with accepted academic practice. No use, distribution or reproduction is permitted which does not comply with these terms.